MEDWIN PUBLISHERS
Committed to Create Value for Researchers

Physical Science & Biophysics Journal
ISSN: 2641-9165

A Tale of the Scattering Lifetime and the Mean Free Path

Contreras P[1]* and Osorio D[2]

[1]Department of Physics, University of the Andes, Venezuela

[2]Department of Brain and Behavioral Sciences, University of Pavia, Italy

***Corresponding author:** Pedro Contreras, Department of Physics, University of the Andes, Mérida, Venezuela, Email: pedrocontre@gmail.com

Research Article

Volume 6 Issue 2

Received Date: November 22, 2022

Published Date: December 30, 2022

DOI: 10.23880/psbj-16000225

Abstract

The idea of applying the scattering lifetime calculated from the imaginary part of the zero temperature elastic scattering cross-section to study a hidden self-consistent damping in two spaces of importance for non-equilibrium statistical mechanics is proposed. It is discussed its relation with the classical phase space from statistical mechanics and the configuration space from nonrelativistic quantum mechanics. This idea is contrasted with the mean free path values in three elastic collision regimes. The main exercise is to study the behavior of a self-consistent probabilistic distribution function in a space we have called the reduced phase space since it is related to the scattering lifetime. This exercise has been solved in two unconventional superconductors for which several calculations are discussed. One of them is to obtain the scattering phase shift from the inverse strength of an atomic potential and the other is to build several phases with different nodal configuration of the superconducting order parameter and show that the imaginary self-consistent part of the scattering cross-section is always positive for two compounds: the triplet strontium ruthenate and the singlet doped with strontium lanthanum cuprate when three models of superconducting order parameters are used: the quasi-point, the point and the line nodal cases. We finally compare the frequency dispersion in the anomalous skin effect with singular shapes of the Fermi surface with the frequency dispersion in the scattering lifetime and their respective mean free paths. This idea is useful because it intuitively explores the nonlocality of this type of hidden self-consistent damping for those incoherent fermionic quasiparticles.

Keywords: Reduced phase space; Configuration space; Classical phase space; Mean free path; Collision lifetime; Damping; Non-equilibrium statistical mechanics

Introduction

This work is aimed at phenomenologically understanding the role of two parameters widely used in non-equilibrium statistical mechanics, the mean free path "*l*" and the scattering lifetime "τ". One calculated and the other used in the study of the elastic scattering cross-section "σ", Both parameters are inversely proportional to "σ" [1-3] (see also Figure 1 for a graphical abstract) in two unconventional superconductors (strontium ruthenate [4,5] and doped with strontium lanthanum cuprate [6-8]) where unconventional superconductivity is suppressed by a nonmagnetic potential following the Larkin equation [9]. These compounds possess different nodal structures that belong to different point group representations. In addition, both compounds have similar crystal structures although they have different stoichiometric/doped composition of the nonmagnetic "strontium" in their elementary crystal cells [10-14].

We illustrate the idea by showing some data calculated self-consistently and address several macroscopic properties that appear numerically, scanning the behavior of the inverse

collision lifetime " τ^{-1} ". It is formalized and explored what we call "the reduced phase space" (RPS), used in this particular case for dressed fermion quasiparticles that are called incoherent carriers following a dependence on the doping concentration (see for example [15]). All this is made with a first neighbors tight-binding procedure. These incoherent carriers obey the Fermi-Dirac statistics and their scattering lifetime strongly depends on the Fermi energy value and the anisotropic Fermi surface average.

Understand the input frequency window that are needed for the calculations in the reduced phase space is crucial and plays a fundamental role since the study of the imaginary part of the scattering cross-section is a well-established methodology [16,17] and it is an instructive computational tool that helps to understand the numerical relation between the macroscopic and microscopic interpretations of different physical phenomena when nonmagnetic disorder is added for the two crystals in their superconducting phases.

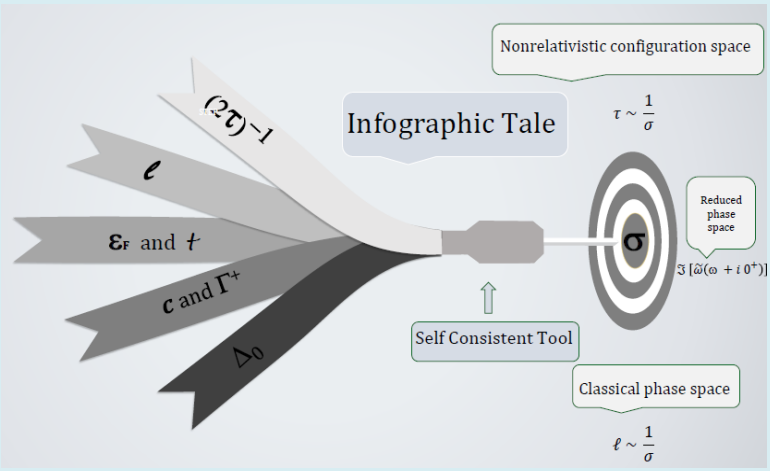

Figure 1: An Infographic Tale of the 2 Physical Parameters.

The numerical disorder is added with the help of two parameters [18]: The dimensionless collision parameter $c = 1/(\pi N_F U_0)$ where U_0 is an impurity atomic potential and N_F is the density of states at the Fermi level. The other parameter is the amount of doping $\Gamma^+ = n_{imp}/(\pi^2 N_F)$ where n_{imp} is the impurity concentration. The reduced phase space (RPS) found, maps a self-consistent distribution probability function always positive for the dressed fermion quasiparticles (incoherent carriers) in the two mentioned compounds in their superconducting phase as it will be shown below.

On the other hand, the non-equilibrium statistical mechanics makes use of the parameters "*l*" and "τ"; for example, for a gas of dressed Fermi quasiparticles. The play between these two parameters, makes it possible to move from a complete description of a non-equilibrium state to an abbreviated description using a single distribution function of one quasiparticle as the one we have obtained [19]. Collision elastic regimes for fermionic dressed quasiparticles depending on the type of collision in the function $\Im\left[\tilde{\omega}\left(\omega + i0^+\right)\right]$ due to nonmagnetic impurities are three [20]:

- The unitary collision regime with a maximum in $\Im\left[\tilde{\omega}\left(\omega + i0^+\right)\right]$ at zero frequency where holds the relation $k_F \sim 1\, a^{-1} \sim 1$ and the mean free path is "l" with $l \sim a$ and is obtained from $l\ k_F \sim 1\, a^{-1} \sim 1$. "$\tilde{\omega}$ – is the self-consistent frequency", "ω – is the real frequency", "$\mathbf{k}_F$ is the Fermi momentum" and "a – is the constant lattice parameter".
- The intermediate collision limit with a nonzero minimum in the imaginary function at the center of the distribution function and two maxima at real frequencies different from zero, where the inequalities $\omega \leq \tau(\tilde{\omega})^{-1}$ and $l \geq a$ take place.
- The hydrodynamic (Born) collision scattering with a null imaginary function at zero frequency and two maxima in the imaginary part at finite real frequencies following the inequalities $\omega \ll \tau^{-1}$ and $l \gg a$ and where self-consistency can be neglected at very low frequencies.

In this work, the physical parametrization of the RPS is made with the help of five physical parameters: the superconducting energy gap at zero temperature " Δ_0 (meV)",

the inverse of the scattering strength "c" (dimensionless parameter), the concentration of non-magnetic impurities "Γ^{+}(meV)", the Fermi energy of the dressed quasiparticles (incoherent carriers) "ε_F (meV)" and the first neighbor hoping tight-binding parameter "t (meV)". Therefore, this is a tight-binding case that generalizes the isotropic case [18,21] adding numerical anisotropy and dispersion in energy (see Figure1 for a graphical abstract). The idea of using four physical parameters self-consistently (Δ_0, ε_F, c and Γ^{+}) as a modeling tool in disordered HTSC was introduced and pointed out by Profs. J. Carbotte and E. Schachinger using isotropic Fermi surfaces in a series of works (check [18,22] and references therein).

The body of this manuscript is as follows. Section 2 introduces the reduced phase space. Section 3 analyzes the sign of the imaginary self-consistent function and the meaning of a hidden damping, additionally links the reduced phase space with the phase spaces of nonequilibrium statistical mechanics and configuration space of nonrelativistic quantum mechanism; and finally; uses numerical values from the self-consistent procedure to build several phenomenologically disordered phase diagrams for the strontium doped $La_{2x}Sr_xCuO_4$, and the triplet Sr_2RuO_4. Section 4 calculates the values for the scattering phase-shift in these compounds using the RPS analysis of the previous section. Section 5 compares briefly the frequency, mean free path and collision scattering lifetime of these two unconventional superconductors with those used in the anomalous skin effect with singular shapes in the Fermi surface for normal metals, and shortly addresses the difficult mathematical issue of nonlocality in "*l*" and "τ". Finally, conclusions and recommendations are given.

The Role of the "Reduced Phase Space" Between Non-Equilibrium Statistical Mechanics and Nonrelativistic Quantum Mechanics

The two dimensional self-consistent reduced phase space (RPS) for dressed fermions (incoherent carriers) is built with the pair of coordinates $(\Re(\tilde{\omega}), \Im(\tilde{\omega}))$ and has the following properties:

- **Property 1:** "The reduced phase space (RPS) in the unitary, intermedium and Born limits has two axis: the real axis $\Re\left[\tilde{\omega}\left(\omega+i0^{+}\right)\right]=\omega$ and the imaginary axis $\Im\left[\tilde{\omega}\left(\omega+i0^{+}\right)\right]$. It serves to map a distribution function of dressed fermion quasiparticles, therefor is a fermionic space (also could be called incoherent phase space).
- **Property 2:** "Unconventional superconductors [17,23] can be also defined as those with nodes/quasinodal regions around the Fermi surface with an order parameter that has a spin paired dependence (singlet or triplet). This property allows to build self-consistently different macroscopic phases as happen for the isotope ^{3}He.
- **Property 3:** "The real part $\Re\left[\tilde{\omega}\left(\omega+i0^{+}\right)\right]$ belongs to the x interval $\in(-\infty,+\infty)$, and the imaginary part only to the positive y axis $\in(0,+\infty)$ with the function $\Im\left[\tilde{\omega}\left(\omega+i0^{+}\right)\right]>0$ always".
- **Property 4:** "The reduced phase space resembles a space where damping is contained in the self-consistent imaginary part of the elastic scattering cross-section following a relationship that holds between the damping and the imaginary part: $\gamma=-\Im\left[\tilde{\omega}\left(\omega+i0^{+}\right)\right]$".

The units for the input and output parameters in the reduced phase space are the rationalized Planck units where always hold that $\hbar = k_B = c = 1$ and input and output units are in in milielectronvolts (meV).

Finally, if is incorporated the tight-binding method (TB) [24] into the dispersion law, the order parameter and the Fermi surface average, considering the group symmetry properties (such as parity and time reversal symmetries), the RPS opens a window to understand some macroscopic properties in these two compounds. Worthy to notice, that the use of the tight-binding enriches but also complicates the computational level of the self-consistent procedure to find the fermionic reduced phase space distribution function, making it more computing demanding.

The Sign of the Imaginary Elastic Cross-Section for Dressed Fermion Quasiparticles

The inverse of the scattering lifetime is given in normal metals and unconventional superconductors by the following expresion $\tau^{-1}(\omega)=2\left[\tilde{\omega}\left(\omega+i0^{+}\right)\right]$ [16,17]. In general, the mathematical treatment of an external constant potential "U_0" using the elastic scattering theory in nonrelativistic quantum mechanics is a complicated subject [25]. In this work, the real part is given in the RPS with the coordinate $\Re(\tilde{\omega})=\omega$. The imaginary term in the RPS is represented by the function $\Im\left[\tilde{\omega}(\omega)\right]=(2\tau)^{-1}\left[\tilde{\omega}(\omega)\right]$ with a hidden self-consistent damping $\gamma=-\Im\left[\tilde{\omega}\left(\omega+i0^{+}\right)\right]$.

Now, let us bring to the attention some examples that address this issue. In first instance, to describe *"self-consistent damping"* in the classical phase space of the non-equilibrium

statistical mechanics (NESM), we need the time-dependent distribution function "*f(t)*" using the τ-approximation in the Boltzmann equation, where the partial derivative respect to time refers to the collision of dressed fermion quasiparticles [26] with $\left(\partial f/\partial t\right)_{coll} = -(f-f_0)/\tau$. If the distribution function goes rapidly to an equilibrium situation denoted by the function , the previous expression can be approximated by

$$(\partial f/\partial t)_{coll} + 2\left[\tilde{\omega}\left(+i0^{+}\right)\right](f-f_0) = 0\,, \qquad (1)$$

with a hidden self-consistent collision *"coll"* behavior and a damping $\gamma = -\Im\left[\tilde{\omega}\left(\omega+i0^{+}\right)\right] = -(2\tau)^{-1}\left[\tilde{\omega}\left(\omega\right)\right]$. The solution of Equation 1 for *(t)* will depend on the whole set of TB parameters Δ_0, ε_F, c, t and Γ^{+}.

A second example, comes from the configuration space in non-relativistic quantum mechanics (NRQM) [27,28]. If the equation for the time dependent probability density $\mathcal{W}(t)$ is obtained with a wave function containing an extra exponential term which describes some damping at the quasi-stationary level. This can happen for one dressed quasiparticle inside an isotropic or anisotropic Fermi reservoir as suggested in [27]. The wave function will contain quasi-stationary levels of the form $\psi_{\omega}(t) \sim e^{-\frac{i}{\hbar}(\epsilon - i\Gamma)t}$. For fermionic quasiparticles is known that $\Gamma/\hbar = (2\tau)^{-1}$ [29] with a probability density $\mathcal{W}(t) = \left|\psi_{\omega}(t)\right|^2 = \mathcal{W}_0 e^{-2\Gamma/\hbar t}$ where $\mathcal{W}_0$ denotes the equilibrium case.

For $\mathcal{W}(t)$ in the configuration space [28], the following equation holds $\partial\mathcal{W}(t)/\partial t = -2\Gamma/\hbar\,\mathcal{W}(t)$ [27]. If we again look at Equation 1 and rearrange this new expression as a partial differential equation with $\Gamma/\hbar = (2\tau)^{-1} = \left[\tilde{\omega}\left(+i0^{+}\right)\right]$, we obtain

$$\left(\partial\mathcal{W}(t)/\partial t\right)_{qsd} + 2\Im\left[\tilde{\omega}\left(\omega+i0^{+}\right)\right]\mathcal{W}(t) = 0, \qquad (2)$$

where now *"qsd"* means quasi-stationary damping, and the time partial derivative refers to quasi-stationary levels such as those that can be originated in an unconventional superconductor with strontium from the influence of its nonmagnetic atomic potential U_0. Equations 1 and 2 are identical although refer to different physical processes (collision and damping). However, Equation 2 resembles the τ-approximation in the kinetic Boltzmann equation, but for NRQM. Henceforth, we can define a hidden damping from Equation 2 as being given by a coefficient $\gamma = -\Im\left[\tilde{\omega}\left(\omega+i0^{+}\right)\right]$ where on the self-consistent mechanism depends how long will survive the dressed quasiparticle (incoherent state) around the atomic potential. We control the physical phases in the RPS by learning how to use properly the five parameters: the number of dressed fermions, the hoping, the strength of the scattering, the zero superconducting gap and the disorder.

Now is clear that this analogy links the quasi-stationary probability density $\mathcal{W}(t)$ on the configuration space [28] and the quasi-stationary distribution function *f(t)* on the phase space [27], one being a classical phenomenon, the other a quantum one (see Figure1). We now understand why is called a "reduced phase space". The answer we find is that the *"lifetime"* is the only output parameter, and the *"mean free path"* has to be given by the strength "c" of the strontium atomic potential as an input dimensionless number, and looking and the distribution functions obtained from the imaginary part, several phases can be predicted.

Non-equilibrium "classical or quantum" statistical mechanics refers also to phenomena where the damping is hidden self-consistently in the distribution probability function *f(t)* or the quasi-stationary probability density , near the equilibrium and with a coefficient

$$\gamma\left[\tilde{\omega}\left(\omega+i0^{+}\right)\right] = -\Im\left[\tilde{\omega}\left(\omega+i0^{+}\right)\right] < 0\,. \qquad (3)$$

Relation (3) means that the imaginary part of the elastic scattering cross-section is always positive defined and can open the possibility for the quasi-nodal points in the OP such as the ones in the Miyake-Narikiyo model [12] where four superconducting isolate quasinodal points are symmetrically distributed in the first Brillouin zone. A second condition in the zero temperature imaginary elastic cross-section is derived from the first

$$\Im\left[\tilde{\omega}\left(\omega+i0^{+}\right)\right] > 0\,. \qquad (4)$$

In order to validate relation (4) in the case of the two unconventional superconductors, we discuss several calculations in detail.

We begin with Table 1 showing a few points of the whole set of data calculated self-consistently to obtain the Miyake-Narikiyo tiny gap [30] in the unitary collision regime with the five input values Δ_0 = 1.0 meV, ε_F = -0.4 meV, c = 0, t = 0.4 meV

and Γ^{+}= 0.05 meV. As can be seen from the second column in Table 1 with values taken from the self-consistent solution for the function $0 \sim -\varepsilon_F + |p_x| v$, the numbers that represent the tiny gap are close to zero but always positive (since 1 meV = 10^{-3} eV), so the values of the imaginary self-consistent elastic scattering cross-section are never zero or negative in our calculations when the Fermi energy is negative and very small (ε_F = - 0.4 meV). The smallest number obtained self-consistently is shadowed gray in the second column of Table 1.

To complement this, some numbers for the case where Sr_2RuO_4 has point nodes is also showed in the third column of Table 1 [31]. The parameter for the Fermi energy is now bigger and close to the zero value (ε_F = - 0.04 meV), but the other four TB parameters remain equal to those used in the quasinodal case. For the node points situation (Figure 2), there are not small values in the imaginary part as seen in the third column of Table 1 and in Figure 2, with the minimum of the imaginary function shadowed gray for a dilute coalescent Γ^{+} = 0.05 meV.

At this point is good to remember that the Fermi-Dirac distribution describes the function of dressed electrons and holes on the quasi-stationary quantum energy levels (e_n and where n = 0,1,2...) with $f_n = 1 \Big/ (e^{\frac{\varepsilon_n - \varepsilon_f}{k_B T}} + 1)$. Therefore, it is important to recall that the Fermi energy ε_F enters as a parameter in the function f_n, and that the consequence of increasing the number of dressed fermion quasiparticles in the system results in an increase of the Fermi energy [32] as we do to obtain point-nodes in strontium ruthenate [31]. Despite strontium ruthenate continues to be part of an intense discussion with respect to its OP as expressed recently in Curtis M, et al. [33], for the point nodes triplet model in the unitary collision regime, Figure 2 shows the behavior of the function $\Im\left[\tilde{\omega}\left(\omega + i0^{+}\right)\right]$ with parameters: $\mathbb{D}_0$ = 1.0 meV, ε_F = -0.04 meV, c = 0, t = 0.4 meV and varying Γ^{+}≈ (0.05-0.40) meV from dilute to optimal [31]. From Figure 2, it can be observed for example, that only for Γ^{+}= 0.05 meV there is a noticeable change in slope around the frequency value of 1.4 meV (T_c for this compound when samples are clear is around 1.5 Kelvin). The other dressed curves show a smooth minimum displaced to higher frequencies [31].

The case involving the HTSC $La_{2x}Sr_xCuO_4$ is more difficult to obtain numerically because the real frequency window should suffix to locate the normal state-superconducting transition point; and in addition; we cannot extend this procedure to the antiferromagnetic phase. This is due to the existence of gap values that strongly depend on disorder [34,35], and this kind of numerical calculation is a difficult task since it depends on the Fermi energy value (the number of dressed quasiparticles) and is very computing demanding task, with real frequencies in a window of 120 meV to describe properly the whole behavior of the imaginary elastic cross-section part (details of the last statement to be published by the authors in a separate manuscript).

One of the peculiarities with the compound $La_{2x}Sr_xCuO_4$ is that T_c depends on both the concentration of doped ions and the number of CuO_2 layers and makes the use of this procedure a computational challenge where the initial frequency values are not always stable to obtain the hidden self-consistency. Similitudes and differences of the two compounds using this approach with a small frequency window is given in [36,37]. We think of a model composed by a gas of fermionic dressed quasiparticles which obey the Fermi liquid behavior [38].

For $La_{2x}Sr_xCuO_4$ we show Table 2 and Table 3 with some numerical results from [20] for a zero superconducting gap with the value $\mathbb{D}_0$=33.9 meV, ε_F = -0.4 meV, c = 0, t = 0.4 meV and Γ^{+}= 0.05 meV using a linear nodal OP model [10,11]. Notice in Table 2, that the box shaded gray represents the minimum value for the imaginary self-consistent function, which is given in Figure 3 in orange color and represents a coalescent phase where the nonmagnetic strontium atoms stick together in a metallic region and get the quasi-momentum transferred from the dressed Fermi quasiparticles, but only for a very dilute doping with Γ^{+} ≈ (0.01 - 0.05) meV represented in Figure 3 with the yellow and orange curves [20].

In the same Figure 3 is observed a very small displacement of the minimum in the imaginary function $\Im\left[\tilde{\omega}\left(\omega + i0^{+}\right)\right]$ when frequency values are increased. This behavior is notorious in the other compound strontium ruthenate and the varying parameter becomes the zero temperature gap as was obtained in Contreras P, et al. [38]. But to slightly notice the same behavior in the doped lanthanum, for now, we show some values taken from Figure 3 in the third column of Table 3, where we have also shadowed some numerical fluctuations in the real frequency values in gray color at the point where the transition occurs, when scanning the function from dilute to optimal values of the doping Γ^{+}.

If the dressed fermionic quasiparticles momentum is transferred to the strontium atoms in the crystal lattice, sticking together in a coalescing metallic state with an almost constant scattering lifetime for the whole set of real frequencies, it allows to adjust non-equilibrium low temperature data fairly well using the same normal state scattering lifetime, but only if the impurity concentration is low enough with Γ^{+}≈ (0.01 -0.05) meV. This hypothesis was firstly proposed in Rink SS, et al. [39]. In addition, we

were able to fit ultrasound and electronic heat transport data for bulk crystals of strontium ruthenate at very low temperatures with a constant lifetime by properly averaging the kinetic coefficients using tight binding parameters, and making use of the three sheets of the Fermi surface, thanks to what, a self-consistency procedure wasn't required [40,41].

In Figure 4 we give an intuitive sketch located inside the dashed blue rectangle built from Figure 3 on how looks like the superconducting part of the phase diagram in the reduced phase space for $La_{2x}Sr_xCuO_4$. We could make it, interpreting the results from the imaginary part of the zero scattering cross-section and the doping Γ^+ is scanned from light to optimal values in the unitary collision regime [20].

At this point, we remind that all calculations were possible thanks to the fact that we added Edwards disorder. A review of the work in this direction with the original references can be found in Ziman JM [42].

The use of the time dependence (non-equilibrium processes) in both functions *(t)* and mentioned in the previous section is crucial to understand the physical picture underlying this approach, that comes from a well-established methodology as the elastic cross-section analysis [16-18,39] when we look at the numbers obtained in the reduced phase space for the lifetime considering the unitary limit. This remark gives the title of this manuscript.

$\omega = \Re(\tilde{\omega})$ (meV)	8.51e-01	8.61e-01	8.71e-01	8.81e-01	8.91e-01	9.01e-01	9.11e-01	9.21e-01	9.31e-01
$(2t^{-1}) = \Im(\tilde{\omega})$ Quasi-point nodes	8.63e-08	3.49e-08	3.54e-04	1.59e-05	6.25e-07	2.21e-08	5.65e-04	1.87e-05	6.74e-07
$(2t^{-1}) = \Im(\tilde{\omega})$ Point nodes	3.43e-01	3.43e-01	3.43e-01	3.43e-01	3.43e-01	3.43e-01	3.43e-01	3.42e-01	3.42e-01

Table 1: Smallest values of the imaginary elastic scattering cross-section for the miyake-narikiyo quasi-points [30] and the point nodes [31] OP. the parameters used are given in the main text, $\Gamma^+ = 0.05$ milielectronvolts.

$\omega = \Re(\tilde{\omega})$ (meV)	33.66	33.71	33.78	33.81	33.86	33.91	33.96	34.01	34.1
$(2t^{-1}) = \Im(\tilde{\omega})$ line nodes	6.06e-02	5.97e-02	5.86e-02	5.75e-02	5.61e-02	5.47e-02	5.56e-02	5.98e-02	6.33e-02

Table 2: Smallest values of the imaginary elastic scattering cross-section for the line nodes op in the unitary limit with a zero gap D_0 =33.94 meV and coalescent (dilute) doping $\Gamma^+ = 0.05$ meV.

$\tilde{A}^+$ (meV)	0.01	0.05	0.1	0.15	0.2
$\omega = \Re(\tilde{\omega})$ (meV)	33.95	33.91	33.9	33.901	33.801
$(2t^{-1}) = \Im(\tilde{\omega})$ Line nodes (meV)	9.63e-03	5.47e-02	1.19e-01	1.89e-01	2.63e-01

Table 3: displacement in the values of the real and imaginary parts of the elastic scattering cross-section observed for the singlet linear op when the zero superconducting gap is D_0 = 33.94 meV and doping goes from very dilute to an optimal value.

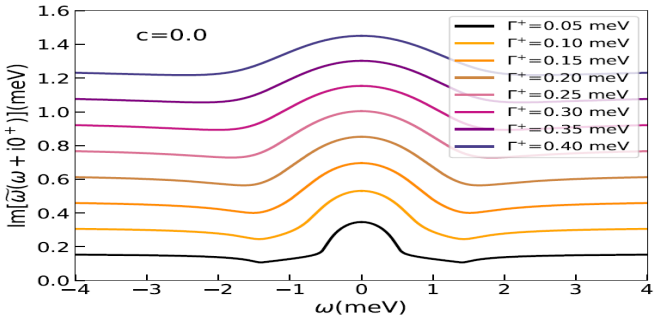

Figure 2: Points Nodes in the Triplet Model When the Fermi Energy is Very Close to Zero. Data in Table 1 Comes from the Black Curve Calculated in Contreras P, et al. [31].

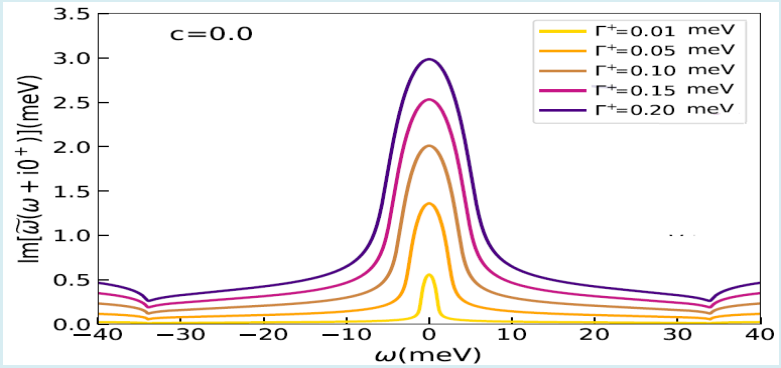

Figure 3: Imaginary Part of the Elastic Scattering Cross-Section in the Unitary Limit for Line Nodes. Data in Table 2 Comes from the Orange Curve [20].

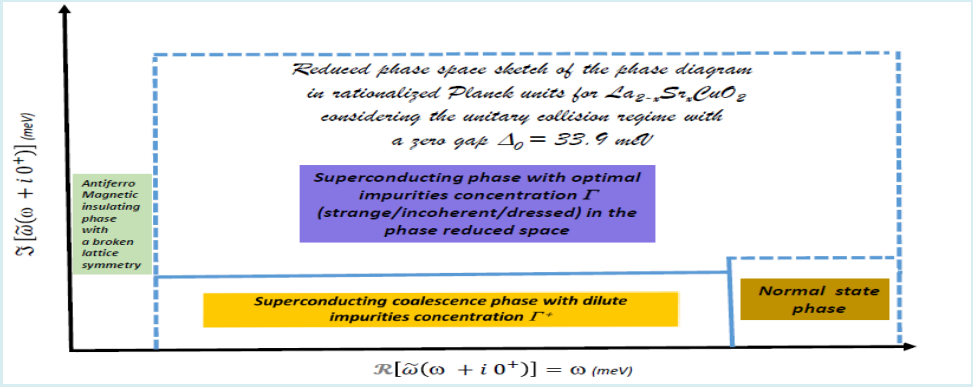

Figure 4: Superconducting Part of The Phase Diagram for Strontium Doped Lanthanum Is Sketched Inside The Blue Dashed Rectangle From The Analysis of Figure3 In The Reduced Phase Space.

The Scattering Phase Shift δ_0 Versus the Inverse Scattering Strength C

Since we used the RPS to numerically calculate self-consistently and study the behavior of several families of positive fermionic distribution functions depending on disorder and scattering strength, that we called in first instance "Wigner macroscopic probabilistic distributions" [43,44] and where the energy is conserved in the three collision regimes, i.e., the unitary, the intermediate and the Born cases. Therefore, we can calculated an important property, "the scattering phase-shift" for the two compounds

using the equation [22] and the results obtained from the set of distribution functions when considering different scattering regimes. Henceforth, we build Table 4 that relates the inverse nonmagnetic dimensionless strength c which the phase shit .

As we can observe from the second column in Table 4, numerically this model shows that the HTSC unconventional superconductor $La_{2x}Sr_xCuO_4$ has a major diversity of phase-shift values than the triplet superconductor strontium ruthenate. This happens when the numerical calculation is performed for the TB values mentioned in section 2 for both compounds since the singlet compound can be numerically found in more regimes, i.e., the unitary, the intermediate and the hydrodynamic limits [20], meanwhile the triplet model remains most of the time in the unitary and intermediate limits.

Strontium ruthenate	c values observed from the imaginary part self-consistently (0.0 for the unitary limit and 0.4 for the intermediate scattering limit) [20]	δ_0 values in degrees calculated for the phase shit from the previous column: 90.00° for the unitary regime and 68.20° for the intermediate scattering limit.
Doped strontium lanthanum cuprate	c values observed self-consistently (0.0 for the unitary limit , 0.2 for the intermediate limit, and 0.4 for the Born regime) [30]	δ_0 values in degrees found for the phase shit from the previous column: 90° for the unitary, 78.70° for the intermediate and 68.20° for the hydrodynamic limit.

Table 4: calculation of the phase shift for both compounds using different regimes for elastic collisions.

Frequency Dispersion Relations for the Anomalous Skin Effect Versus the Elastic Self-Consistent Scattering Lifetime

Finally, in order to gain additional credibility in the use of the RPS approach with respect to the Boltzmann kinetic equation; we conclude with a very short analysis by contrasting frequency values with the anomalous skin effect [45] and the examples discussed in previous sections. We first, give a brief introduction to the anomalous skin effect and after that we assemble Table 5 to summarize section five.

Differences between normal and anomalous skin effects

In the anomalous skin effect, the equation for the metallic impedance changes and the electronic mean free path "l" starts to play a role. Let us, summarize the main differences between the normal and anomalous skin effect briefly to start with [46]. In the normal skin effect, the metallic impedance "ζ" has the equation ζ = Re(ζ) –i Im (ζ) composed by equal real resistive and imaginary reactive terms where Re ζ = Im $\zeta = \sqrt{2\pi\omega / (\sigma c^2)}$. The physical behavior of an external electromagnetic field (EMF) on the metal surface is to penetrate it and decay as $\sim e^{-x/\delta}$ with an effective penetration depth of the EMF given by $\delta_{normal} = c/\sqrt{2\pi\omega\sigma}$ which does not depend on the mean free path [46].

However, normal metals have a high conductivity "σ" when d_{normal} is small, but at low temperatures the mean free path "l" becomes larger and the Ohm law in the local form $j = \sigma E$ cannot be applied. Thus, it is used a non-local equation (*) $j(r) = \int k_{ik}(r, r') E_k(r') dr'$ where the anomalous skin effect is defined by saying that the kernel of the equation (*) depends on the mean free path "$k_{ik}(r, r') \sim$ I" [47]. As a consequence, the external electric field is non-uniform, and since the normal skin effect can be derived from the kinetic equation only if the electric field is assumed uniform, the kinetic equation in the diffusive limit for a non-equilibrium fermionic distribution function has to be solved [47].

The main qualitative difference between normal and anomalous skin effects in the impedance equation is given by the square root of three in the imaginary part of the impedance: ζ = Re(ζ) – $\sqrt{3}$ i Im (ζ). Additionally, the depth penetration has a mean free path dependence given by $\delta_{anomalous} = \sqrt[3]{c^2 l} / \sqrt{4\pi\omega a\sigma}$ with $a \sim 1$, and this dependence between the mean free path "l" and the anomalous penetration depth is used to plot "ζ". Otherwise, normal and anomalous skin effects can be differentiate sketching $(\text{Re}\ \zeta)^{-1}$ versus $\sigma^{1/2}$, where two regions are well defined [46]. One of them where the inverse resistive impedance has an approximate linear dependence on the square root of the conductivity that is the normal skin effect and another where the resistive impedance is constant and is called the anomalous skin effect [46].

Geometrical Interpretation of the Singular Behavior in the Anomalous Skin Effect

To describe the anomalous skin effect in geometrical terms, we say that the anomalous skin effect happens if the fermionic quasiparticles lye in a belt of the Fermi surface with two geometrical conditions: First, $\boldsymbol{n}.\boldsymbol{v}(\boldsymbol{p})=0$ where $\boldsymbol{n}$ is a vector normal to the metallic surface; and; Second $\varepsilon(p)-\varepsilon_F=0$ [48]. The singularities in $\varepsilon(p)$ will become important for the anomalous skin effect region when the radius $\ell/\delta_{normal} \ggg 1$ and that happens when the dispersion law for fermionic quasiparticles has terms of the type $0\sim-\delta_F+|p_x|v$ +(higher order terms in momentum) [48] which is possible if the fermionic quasiparticles obey a non-quadratic energy spectrum. In that case $\boldsymbol{n}.\boldsymbol{v}(\boldsymbol{p})=0$ is not the equation of a plane in the phase space and the belt is not a planar curve [48]. In this case the geometry of the belt is a strong function of the geometry of the Fermi surface and the direction of the vector $\boldsymbol{n}$. As a consequence of this, the type of connectivity changes in two different ways: either a closed loop can appear or disappear in the belt (O-type singularity), or a bridge between two loops can rupture or rejoin (X-type singularity) [49]. As a consequence, non-equilibrium "kinetic" characteristics of a metal such as the anomalous skin effect, or the sound absorption have singularities of the "0" or "X" types and the change in the shape of the belt gives "local information" about the Fermi surface. Kaganov MI and Avanesyan G [48,49] called the *p-point* responsible for this type of change in connectivity *"a critical point p_c"*, and showing that they are located *"along curves of parabolic points"*. Therefore, the singularities of 0 and X types can only occur only for those metals whose Fermi surfaces have parabolic points (called also zero curvature lines [49]).

If the metal is isotropic, then there will be an effective conductivity given by the equation $\sigma_{effective}=ia\sigma/(|k|\ell)$ with $a\sim 1$ because the number of fermion quasiparticles that participate in the anomalous skin effect is approximated by $n_{effective}\sim n\delta/\ell$ [46]. Thus, one can say that the effective conductivity when the Fermi surfaces are isotropic depends on the mean free path as $1/\ell$, i.e., $\sigma_{effective}\propto\sigma/(|k|\ell)$ and depends "only" on the characteristics of the fermionic spectrum [46]. To finalize this brief summary, it is important to mention that the diffusive reflection in the anomalous skin effect is given by including the term $\boldsymbol{v}.\partial f/\partial \boldsymbol{r}$ in the Boltzmann kinetic equation, where $\boldsymbol{v}=f(\boldsymbol{p})$ is the velocity of a fermion quasiparticle with $\boldsymbol{p}$ a quasi-momentum in the crystal lattice [47], that can be mitted only in the case when the mean free path is much smaller than the distances along which the electric field changes significantly, in other words, nonlocality is neglected and the skin effect is in the normal regime when the resistive and reactive parts of the impedance are equal and the conductivity does not depend on the mean free path.

Anomalous Singular Skin Effect "L" versus Incoherent (Dressed)Superconducting "1/ (2τ)"

A link with the previous sections arises naturally because we seek an analogy between the phase and the configuration spaces and the existence of a kernel in the integro-diferential equations that include nonlocality of the kinetic parameters *l* and τ. As pointed out in Kaganov MI, et al. [47] *"to find out the explicit form of the kernel* $\boldsymbol{k}$ *(ik) the kinetic equation for the non-equilibrium part of the electron distribution function must be solved"*. Table 5 shows several frequency dependent dispersion relations for "*l*" and "τ "by comparing the two effects: the anomalous skin effect in normal metals with Fermi surfaces with parabolic points [48], with the reduced phase space for unconventional superconductors. In Kaganov MI, et al. [48], it was found theoretically the impedance in the hydrodynamic limit $\omega\tau\ll 1$ for the anomalous skin effect in thin metallic films by giving some examples using complicated 3D Fermi surfaces to average the conductivity and the impedance. We found that the real part of the impedance strongly depends on two parameters: the mean free path and the shape of the belts on each Fermi surface studied (the shape of the singular belts makes used of the topological generalized Lifshitz transitions [47]).

It was noticed in Kaganov MI, et al. [48] that by doing an appropriate integration, two physical behaviors can be distinguished in the anomalous real part of the impedance (one of them called a singular behavior, check Figure 6 in Kaganov MI, et al. [48] and Table 1 Kaganov MI, et al. [47] for the type of singular points [49] and the impedance dependence on the mean free path). Hence, it was stated in Kaganov MI, et al. [47] that the solution for the impedance and conductivity depend sensitively on the ratio of spatial and temporal dispersions of the kinetic parameters "*l*" and "τ". Therefore, we state in this work, that the solution for the imaginary function $\Im\left[\tilde{\omega}(\omega+i0^+)\right]$ (or the inverse scattering lifetime) depends sensitively on the ratio of spatial and temporal dispersions for "*l*" and "τ" as well, since for the

analysis of the previous sections, we needed the unitary collision limit where the mean free path $l \sim a$, being a the lattice parameter, but requiring this time a self-consistent calculation of the inverse scattering lifetime $1/\tau(\tilde{\omega})$, although it might be no obvious in this case, because the existence of the kernel is not clear.

In addition, the frequency window required in the reduced phase space for the two unconventional superconductors happens if $\omega \sim 1/\tau \sim 4$Ä$_0$ (around 4 meV for strontium ruthenate and 120 meV for the doped with strontium lanthanum cuprate). Moreover, the tight-binding parameters $(t, \grave{o}_F)$ influence strongly the Fermi surface averages and their values are able to distinguish different OP physical phases as it was done by comparing the singular belts in the anomalous skin effect [37]. Therefore, the relation dispersion in the scattering lifetime that holds for the unitary collision regime in the reduced phase space might be written as stated in the introduction.

$$\omega\tau\left(\tilde{\omega}(\grave{u})\right) \sim 1 \tag{5}$$

To conclude, it is important to recall that recently, the anomalous skin effect with this type of anomalies in the Fermi surface has gained attention among the research community. Mainly for microwave applications [50,51] and in the study of nonlocality phenomena in solids, as recently was theoretically and experimental realized for the compound $PdCoO_2$ [52,53].

Kinetical Physics Condensed Matter Phenomena.	To study in:	Theoretical methods of solution	Temporal dispersion relation for the scattering lifetime	Spatial dispersion relation for the quasiparticles
Anomalous skin effect and surface impedance with Fermion quasiparticles.	Normal metal thin samples.	Kinetic Boltzmann Equation in the τ-approximation.	$\omega\tau \ll 1$ Hydrodynamic limit	$l \gg \delta$ δ is the anomalous skin depth, the mean free path is l
Strange metallic phase in two unconventional superconductors	Superconducting ceramic thin samples for the doped HTSC and crystal bulb samples for the ruthenate	Numerical self-consistent equation $\Im\left[\tilde{\omega}\left(\omega + i0^+\right)\right]$ in the reduced phase space.	$\omega\tau\left(\tilde{\omega}(\omega)\right) \sim 1$ Unitary limit	$l \sim a$ a is the lattice parameter

Table 5: Dispersions for the anomalous skin effect versus the two unconventional superconductors.

Conclusion and Recommendations

This work was aimed at introducing with some numerical examples the importance of two physical parameters, the mean free path and scattering lifetime, both widely used in non-equilibrium statistical mechanics and a brief analysis of what we have called the reduced phase space for the real and imaginary parts of the elastic scattering cross-section, using two unconventional superconductors in the unitary limit as examples, when the fermionic quasiparticles are dressed by a non-magnetic impurity potential, for three cases of the order parameter, the quasi/nodes, point nodes and line nodes using a 2D anisotropic TB self-consistent parametrization with nearest neighbor hoping.

Despite, we focused our study to the unitary regime, we took into account a discussion involving three scattering regimes in the imaginary part of the elastic cross-section. We have defined a "*hidden damping parameter*" $\gamma = -\Im\left[\tilde{\omega}\left(\omega + i0^+\right)\right]$ in *"the imaginary part of the elastic scattering cross-section"*, being the last always positive, i.e., "$\Im\left[\tilde{\omega}\left(\omega + i0^+\right)\right] > 0$" obtained using a self-consistent numerical procedure. Therefore, that kind of self-consistent hidden behavior might be of interest for researchers who study the statistical physics of non-equilibrium phenomena (classical or quantum) from a macroscopic point of view.

To conclude, several examples were analyzed in sections 2 to 5. Sometimes using tables and figures from numerical calculations, but also giving analogies between the classical phase space of the non-equilibrium statistical mechanics, the configuration space of nonrelativistic quantum mechanics, and the reduced phase space (see Figure 1 for a graphic summary). The study of the imaginary part of the elastic cross-section not only is important for these two models of unconventional superconductors with strontium, but also is of interest for the study of fermionic and bosonic trapped gases at very low temperatures as it has been addressed [54].

Acknowledgements

This research did not receive any specific grant from funding agencies in the public, commercial, or not-for-profit sectors. We thank an anonymous reviewer of this work to help us to clarify and expand the meaning of section 5 and an anonymous reviewer from a previous publication Contreras P, et al. [38] whose technical questions induced us to write this manuscript. Finally, we acknowledge the effort of Medwin Publishers in the mission of promoting academic exchanges and the advancement of science by helping the most disadvantaged scientists around the world.

References

1. Reif F (1965) Fundamentals of Statistical and Thermal Physics. McGraw-Hill, New York.
2. Pitaevskii LP, Lifshitz E, Sykes J (1981) Physical Kinetics. 1st(Edn.), Pergamon.
3. Dorfman JR, Beijeren HV, Kirkpatrick TR (2021) Contemporary Kinetic Theory of Matter. Cambridge University Press, USA.
4. Maeno Y, Hashimoto H, Yoshida K, Nishizaki S, Fujita T, et al. (1994) Superconductivity in a layered perovskite without copper. Nature 372: 532-534.
5. Rice TM, Sigrist M (1995) Sr_2RuO_4: An electronic analogue of 3He? Journal of Physics: Condensed Matter 7(47): L643-L648.
6. Bednorz J, Müller K (1986) Possible high Tc superconductivity in the Ba-La-Cu-O system. Zeitschrift fur Physik B Condensed Matter 64: 189-193.
7. Bednorz JG, Müller KA (1988) Perovskite-type oxides-The new approach to High-Tc superconductivity. Rev Mod Phys 60(3): 585.
8. Kastner MA, Birgeneau RJ, Shirane G, Endoh Y (1998) Magnetic, transport, and optical properties of monolayer copper oxides. Rev Mod Phys 70(3): 897.
9. Larkin A (1965) Vector pairing in superconductors of small dimensions. JETP Letters 2(5): 105.
10. Scalapino DJ (1995) The case for dx2 − y2 pairing in the cuprate superconductors. Physics Reports 250(6): 329-365.
11. Tsuei CC, Kirtley JR (2000) Pairing symmetry in cuprate superconductors. Reviews of Modern Physics 72: 969.
12. Miyake K, Narikiyo O (1999) Model for Unconventional Superconductivity of Sr_2RuO_4, Effect of Impurity Scattering on Time-Reversal Breaking Triplet Pairing with a Tiny Gap. Phys Rev Lett 83: 1423.
13. Walker MB, Contreras P (2002) Theory of elastic properties of Sr_2RuO_4 at the superconducting transition temperature. Physical Review B 66(21): 214508.
14. Sigrist M (2002) Ehrenfest relations for ultrasound absorption in Sr_2RuO_4. J Phys Soc Japan 107 (5): 917-925.
15. Putzke C, Benhabib S, Tabis W, Ayres J, Malone L, et al. (2021) Reduced Hall carrier density in the overdoped strange metal regime of cuprate superconductors. Nat Phys 17: 826-831.
16. Pethick CJ, Pines D (1986) Transport processes in heavy-fermion superconductors. Phys Rev Lett 57(1): 118-121.
17. Mineev V, Samokhin K (1999) Introduction to Unconventional Superconductivity. Gordon and Breach Science Publishers, USA.
18. Schachinger E, Carbotte JP (2003) Residual absorption at zero temperature in d-wave superconductors. Phys Rev B 67: 134509.
19. Kaganov MI, Lifshitz IM (1989) Quasiparticles: Ideas and Principles of Quantum Solid State Physics. 2nd(Edn.), MIR Publishers, Moscow, Russia.
20. Contreras P, Osorio D (2021) Scattering Due to Non-magnetic Disorder in 2D Anisotropic d-wave High Tc Superconductors. Engineering Physics 5(1): 1-7.
21. Contreras P, Moreno J (2019) Nonlinear minimization calculation of the renormalized frequency in dirty d-wave superconductors. Can J Pure Appl Sci 13(2): 4807-4812.
22. Schurrer I, Schachinger E, Carbotte b JP (1998) Optical conductivity of superconductors with mixed symmetry order parameters, Physica C Superconductivity and its Applications 303(3): 287-310.
23. Annett JF (2004) Superconductivity, Superfluids, and Condensates. Oxford Master Series in Physics, Oxford university press, USA.
24. Harrison WA (1980) Electronic Structure and Properties of Solids. Dover, pp: 582.
25. Landau LD, Lifshitz EM (1981) Quantum Mechanics: Non Relativistic Theory. 3rd(Edn.), Butterworth-Heinemann, pp: 689.
26. Blatt F (1957) Theory of mobility of electrons in solids. Solid State Physics 4: 199-366.
27. Kvashnikov I (2003) The theory of systems out of equilibrium. Moscow State University Press, Russia, 3.

28. Davydov AS (1965) Quantum Mechanics. Pergamon Press, pp: 680.

29. Schrieffer J (1970) What is a quasiparticle? Journal of Research of the National Bureau of Standards 74A (4): 537-541.

30. Contreras P, Osorio D, Ramazanov S (2022) Non-magnetic tight binding disorder effects in the γ sheet of Sr_2RuO_4. Rev Mex Fis 68(2): 1-5.

31. Contreras P, Osorio D, Tsuchiya S (2022) Quasi-point versus point nodes in Sr_2RuO_4: The case of a flat tight binding γ sheet. Rev Mex Fis 68(6): 1-8.

32. Brandt NB, Chudinov SM, (1975) Electronic structure of metals. MIR Publishers, India.

33. Curtis M, Gradhand M, Annett J (2022) Uniaxial strain, topological band singularities and pairing symmetry changes in superconductors. arXiv, Superconductivity.

34. Yoshida T, Malaeb W, Ideta S, Fujimori A, Lu DH, et al. (2012) Coexisting pseudo-gap and the superconducting gap in the High-Tc La_2-xSrxCuO_4. Journal of the Physical Society of Japan 81: 011006.

35. Contreras P, Osorio D, Beliayev EY (2022) Dressed behavior of the quasiparticles lifetime in the unitary limit of two unconventional superconductors, Low Temp Phys 48(2): 187-192.

36. Contreras P, Osorio D, Beliayev E (2022) Tight-Binding Superconducting Phases in the Unconventional Compounds Strontium-Substituted Lanthanum Cuprate and Strontium Ruthenate. American Journal of Modern Physics 11(2): 32-38.

37. Walker MB (2001) Fermi-liquid theory for anisotropic superconductors. Phys Rev B 64(13) 134515.

38. Contreras P, Osorio D, Devi A (2022) The effect of nonmagnetic disorder in the superconducting energy gap of strontium ruthenate. Physica B: Condensed Matter 646: 414330.

39. Rink SS, Miyake K, Varma C (1986) Transport and thermal properties of heavy-fermion superconductors: A unified picture. Phys Rev Lett 57: 2575.

40. Contreras P, Walker MB, Samokhin K (2004) Determining the superconducting gap structure in from sound attenuation studies below Tc. Phys Rev B 70(18): 184528.

41. Contreras P (2011) Electronic heat transport for a multiband superconducting gap in Sr_2RuO_4. Rev Mex Fis 57(5): 395-399.

42. Ziman JM (1979) Models of Disorder: The Theoretical Physics of Homogeneously Disordered Systems. 1st(Edn.), Cambridge University Press, United Kingdom, pp: 542.

43. Wigner EP (1932) On the quantum correction for thermodynamic equilibrium. Phys Rev 40(5): 749-759.

44. Carruthers P, Zachariasen F (1983) Quantum collision theory with phase-space distributions. Rev Mod Phys 55(1): 245-285.

45. Reuter GEH, Sondheimer HE (1948) The theory of the anomalous skin effect in metals. Proceedings of the Royal Society of london 195(1042): 336-364.

46. Abrikosov A (1972) Introduction to the theory of normal metals. Academic Press Inc, pp: 293.

47. Kaganov MI, Lyubarskiy G, Mitina A (1997) The theory and history of the anomalous skin effect in normal metals. Physics Reports 288(1-6): 291-304.

48. Kaganov MI, Contreras P (1994) Theory of the anomalous skin effect in metals with complicated Fermi surfaces. Journal of Experimental and Theoretical Physics 79(6): 985-986.

49. Avanesyan G, Kaganov MI, Lisovskaya T (1977) Metal phonon-spectrum singularities determined by local geometry of the Fermi surface. JETP Letters 25(8): 355-357.

50. Torkhov N, Babak L, Kokolov A, Sheyerman F (2019) The influence of fractal geometry on anomalous skin-effect in metal systems. 29th International Crimean Conference "Microwave & Telecommunication Technology" 30: 1-6.

51. Torkhov NA, Babak LI, Budnyaev VA, Kareva KV, Novikov VA (2022) Conversion of the anomalous skin effect to the normal one in thin-film metallic microwave systems. Phys Scr 97(9).

52. Baker G (2022) Non-local electrical conductivity in $PdCoO_2$. University of British Columbia, USA.

53. Baker G, Branch TW, Day J, Valentinis D, Mohamed Oudah, et al., (2022) Non-local microwave electrodynamics in ultra-pure $PdCoO_2$. arXiv:2204.14239.

54. Pitaevskii LP (2008) Superfluid Fermi liquid in a unitary regime. Phys Usp 51: 603.